Available online at www.sciencedirect.com
SCIENCE DIRECT®
Journal of Photochemistry and Photobiology A: Chemistry 163 (2004) 171–180
Journal of Photochemistry and Photobiology A:Chemistry
www.elsevier.com/locate/jphotochem

Spectral and photophysical properties of some imidazo[1,2-*a*]purine derivatives related to acyclovir

G. Wenska [a,*], J. Koput [a], M. Insinska-Rak [a], B. Golankiewicz [b], T. Goslinski [b], T. Ostrowski [b]

[a] *Faculty of Chemistry, Adam Mickiewicz University, Grunwaldzka 6, 60-780 Poznan, Poland*
[b] *Institute of Bioorganic Chemistry, Polish Academy of Sciences, Noskowskiego 12/14, 61-704 Poznan, Poland*

Received 21 August 2003; received in revised form 5 November 2003; accepted 20 November 2003

Abstract

Spectral and photophysical properties of 3,9-dihydro-3-[(2-hydroxyethoxy)methyl]-6-phenyl-9-oxo-imidazo[1,2-*a*]purine **7b** (congener of acyclovir) and its three substituted derivatives **7a**, **c** and **8a** in organic solvents and in aqueous buffer solutions have been determined. Compound **7c** has an ester group in the *para* position of the phenyl ring, compounds **7a** and **8a** are derivatives of **7b** with a methyl group attached to imidazole N(5) or pyrimidine N(4) ring of the tricyclic skeleton, respectively. Experimental study has been supplemented with theoretical calculations of the singlet electronic transition energies and oscillator strengths by the time dependent density functional theory (TD-DFT). Combination of experimental and computational results have indicated that compounds **7b** and **c** having mobile hydrogen exist in the ground state in a single N(5)*H* tautomeric form. The lowest excited S_1 state of all compounds investigated has the π, π^* configuration. The spectral and photophysical properties of **7a**–**c** are similar. The fluorescence behaviour of the compounds depends on the solvent polarity and pH of the aqueous medium in the range of pH: 0–4 and 6–12. The pH dependence is a consequence of the protonation of the molecules ($pK_a = 2.2$ for **7a** and $pK_a = 2.0$ for **7b** and **c**) and their deprotonation in the ground state ($pK_a = 8.0$ and 8.2 for **7b** and **c**, respectively). The absorption and fluorescence properties of the ionic forms have been determined. In contrast to **7a**–**c**, the spectral and photophysical properties of **8a** are not significantly influenced by the solvent polarity and they are independent on pH of aqueous solution within 4–12 range.

Keywords: Fluorescence; Absorption; Acyclovir derivatives; Imidazo[1,2-*a*]purine

1. Introduction

The derivative of 6-methyl-9-oxoimidazo[1,2-*a*]purine bearing a hydroxyethoxymethyl (hem) substituent at N(3) position, compound **1** (Scheme 1), has been proved markedly and selectively active against herpes viruses [1]. Because the compound **1** is structurally related to the guanine-derived acyclovir (9-[(2-hydroxyethoxy)methyl]guanine), and both exhibit similar biological activity, in literature the former is referred to as tricyclic analogue of acycolvir. The other derivatives of tricyclic heteroaromatic system: the compounds **2**–**6** presented in Scheme 1, are antivirally inactive. Nevertheless, two of them, namely ribosides: 1,N^2-ethenoguanosine, **2** (3,9-dihydro-9-oxo-3-(β-D-ribofuranosyl)-imidazo[1,2-*a*]purine, Scheme 1) and wyosine, **3** (4,9-dihydro-4,6-dimetyl-9-oxo-3-(β-D-ribofuranosyl)-imidazo[1,2-*a*]purine, Scheme 1) are of biological relevance.

Compound **2** is formed in DNA as a result of a reaction of metabolites of the known carcinogen—vinyl chloride—with guanosine residues [2,3]. Wyosine, **3**, occurs naturally in some tRNAs [4]. Despite structural similarity of the compounds the properties of their S_1 excited states differ, because nucleoside **3** and acyclonucleoside **4** [5], as opposed to compounds **1** and **2** and the synthesised compounds **5** and **6** (Scheme 1) [1,6], emit blue fluorescence at room temperature [4,7,8]. It has been suggested that the attachment of a methyl group to the nitrogen of the central pyrimidine ring, which locks the tricyclic chromophoric system in N(4)*H* tautomeric form is responsible for the appearance of fluorescence [2]. However, so far the absorption and fluorescence properties of the compounds shown in Scheme 1 have not been studied comprehensively. The absorption spectra or parameters characterising the absorption properties of the compounds in a single solvent, usually water at pH 7, have been reported [1,2,5,6]. The emission studies have been limited to

* Corresponding author. Tel.: +48-61-829-13-51; fax: +48-61-865-80-08.
E-mail address: gwenska@amu.edu.pl (G. Wenska).

1010-6030/$ – see front matter © 2003 Elsevier B.V. All rights reserved.
doi:10.1016/S1010-6030(03)00444-1

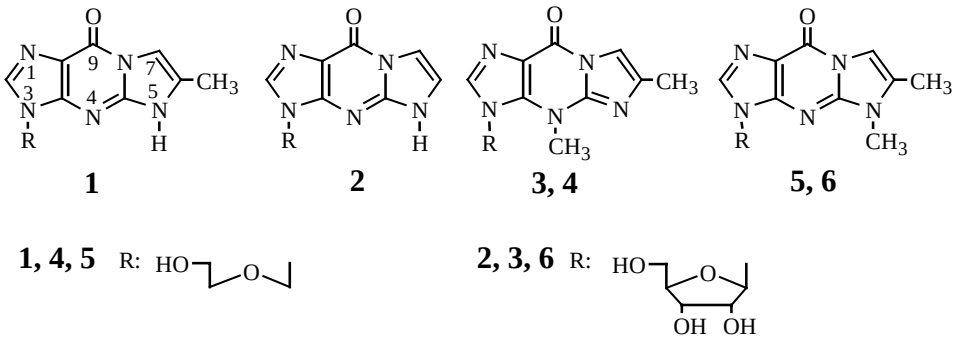

Scheme 1.

a measurement of the fluorescence decay of the nucleoside **3** in DMSO solution at room temperature [7]. Fluorescence of the aglycone of the nucleoside **3**, i.e. wye base (4,9-dihydro-4,6-dimethyl-9-oxo-imidazo[1,2-*a*]purine), which contains hydrogen atom at N(1) position of the tricyclic system instead of ribosyl present at the N(3) site in nucleoside **3**, has been studied in more detail [9–11]. However, the fluorescence properties of the wye base and nucleoside **3** are not compatible since both compounds represent different tautomeric forms of the parent chromophoric system.

A combination of biological activity and fluorescent property of a compound is of interest because the emission can be employed for monitoring of the drug in biological fluids or its detection in tissues [12]. In the systematic approach directed towards developing a drug with this property, it has been found that an introduction of an aryl substituent into the C(6) position of compound **1** makes the resulted compounds **7b** and **c** (Scheme 2) fluorescent and improves their biological activity, particularly this of **7c** [13–16].

The aim of the study reported was to characterise the absorption and fluorescence properties of compounds **7b** and **c** in media of different polarity and as a function of pH in aqueous solution. The study was extended to two methylated derivatives of **7b**, namely compounds **7a** and **8a**. The regioisomers, being models of N(4)*H* and N(5)*H* tautomers of **7b** locked by methyl group, appeared to be helpful in elucidating the properties of the latter compound in the ground and excited electronic states. All the compounds were subjected to absorption, steady-state and dynamic fluorescence studies. The experimental results were supplemented by calculations of singlet excited states properties of **7a**′, **b**′, and **8a**′, **b**′ relevant for the study. The structures of the compounds investigated are presented in Scheme 2.

2. Experimental

2.1. Materials

The compounds **7a–c** and **8a** were synthesised according to earlier published procedures [13–15]. To remove any emitting impurities the samples were purified by HPLC (Waters 600 E) equipped in Waters 991 Photodiode Array Absorption Detector and Waters 470 Scanning Fluorescence Detector. The HPLC analyses were carried out on a reversed phase column (X-Terra RP_{18}, 3.5 μm × 4.5 mm × 150 mm) using CH_3CN–H_2O mixture as an eluent. The pure samples were collected, evaporated under reduced pressure and finally dried over P_2O_5.

Spectroscopic grade (Merck) methanol, *n*-butanol, 1,4-dioxane and HPLC grade acetonitrile (Scharlau) were used as received. The solvents' purity was checked by measuring their absorption and emission spectra. Water was purified by using Millipore Super Q system. Sodium acetate, acetic acid (pH 3.6–5.6), phosphate (pH 5.8–8), boric acid, NaOH (pH 8–10) buffers were used [17]. The acidity

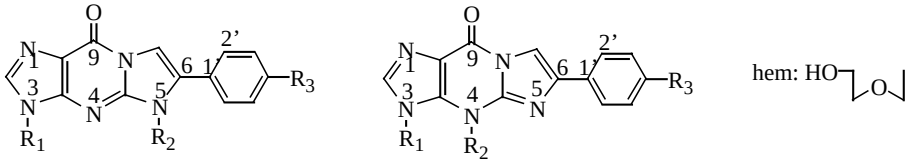

7a: R_1= hem; R_2= CH_3; R_3= H
7a': R_1= CH_3; R_2= CH_3; R_3= H
7b: R_1= hem; R_2=H; R_3= H
7b': R_1= CH_3; R_2= H; R_3= H
7c: R_1= hem; R_2= H; R_3= $OCOCH(CH_3)_2$

8a: R_1= hem; R_2= CH_3; R_3= H
8a': R_1= CH_3; R_2=CH_3; R_3= H
8b': R_1= CH_3; R_2= H; R_3= H

Scheme 2.

and basicity of aqueous solutions in the range pH 3.6–1 and 10–12 was adjusted by using 0.1 M NaOH and 0.1 M HCl. The mixtures H_2O–H_2SO_4 were used below pH 1 [18].

2.2. Methods

The electronic structure of the molecules **7a′**, **b′** and **8a′**, **b′** was studied by means of the time dependent density functional theory (TD-DFT) [19]. The calculations were performed using the hybrid method B3LYP [20] in conjunction with the modest split-valence polarised basis set 6-31G* [21], and by employing the Gaussian package of ab initio programs [22]. The excitation energies and transition intensities were calculated for the optimised ground state geometry of the molecules. Oscillator strengths were calculated in the dipole length representation.

Absorption spectra were recorded with Cary 300 Bio (Varian) spectrophotometer. Corrected fluorescence emission and excitation spectra were recorded using a Perkin-Elmer LS-50B spectrofluorometer. Fluorescence emission from the solvents was found to be insignificant. The concentration of the samples was $\leq 5 \times 10^{-5}$ M. Fluorescence quantum yields were determined using quinine sulphate in 0.05 M H_2SO_4 as a standard ($\phi_F = 0.52$ [23]). Spectral titrations and determination of pK_a were performed as described [18]. Fluorescence lifetimes were measured with an IBH Consultants (Glasgow, Scotland) model 5000 fluorescence lifetime spectrometer using a H_2-filled nanosecond flashlamp as an excitation source. Reconvolution of fluorescence decay curves was performed using the IBH Consultants Version 4 software. The quality of the fit was judged from the χ^2 values ($\chi^2 \leq 1.2$) and random distribution of weighted residuals.

3. Results and discussion

3.1. Theoretical calculations

The energies (E_{calc}) and oscillator strengths (f) of several singlet electronic absorption transitions $S_0 \rightarrow S_n$ in vacuum were computed for the compounds **7b′** and **8b′** representing N(4)*H* and N(5)*H* tautomers of **7b**, and for **7a′** and **8a′** which are analogues of **7a** and **8a**. As follows from the structures presented in Scheme 2, in the calculations the hydroxyethoxymethyl group at the N(3) position of the tricyclic skeleton was replaced by a methyl substituent. The parent molecules **7a′**and **b′** were found to be non-planar in the ground state and the twist angles (the angle 7-6-1′-2′ indicated in Scheme 2) between the heteroaromatic and phenyl rings were calculated to be 42° for **7a′** and 26° for **7b′**. In contrast, the respective isomers: **8a′** and **b′** were found to be essentially planar, with the angle 7-6-1′-2′ being −1° for **8a′** and 0° for **8b′**. As follows from the results presented in Table 1, the first electronic absorption transition in **7b′** (N(5)*H* tautomeric form) occurs at the energy by 3900 cm^{-1} lower than that in **8b′** (N(4)*H* tautomeric form). The replacement of a hydrogen atom in both tautomers by a methyl group does not change significantly the energy and oscillator strength at least for the two lowest energy electronic transitions. For all the compounds investigated the two lowest singlet excited states are separated by ≥4000 cm^{-1}. An analysis of the calculated CI expansion coefficients and molecular orbitals indicates that the lowest energy transition in all molecules investigated is of the π, π* type.

The monoprotonated forms of the compound **7b′** (Scheme 2) were investigated with proton being attached to the atoms N(1), N(4) or N(8). For $N(1)H^+$, $N(4)H^+$ and $N(8)H^+$ species derived from **7b′** the deprotonation energies were calculated at the B3LYP/6-31G* level to be 248.4, 230.2 and 232.8 kcal/mol, respectively.

3.2. Spectral and photophysical properties of 7*a*–*c* and 8*a* in selected solvents

The absorption and emission spectra of the compounds **7a**–**c** and **8a** were measured in either protic: CH_3OH, n-C_4H_9OH or aprotic: CH_3CN, 1,4-dioxane, organic solvents and in aqueous solution pH at 5.8. Weakly acidic aqueous medium has been chosen to avoid deprotonation of **7b** and **c** and to assure that all molecules studied exist exclusively as neutral molecules in the ground state (pK_a

Table 1
Energies (E_{calc}) and oscillator strengths (f) of singlet electronic transitions $S_0 \rightarrow S_n$ of **7a′**, **b′** and **8a′**, **b′** in vacuum[a]

$S_0 \rightarrow$	**7a′**		**7b′**		**8a′**		**8b′**	
	E_{calc} (cm^{-1})	f	E_{calc} (cm^{-1})	f	E_{calc} (cm^{-1})	f	E_{calc} (cm^{-1})	f
S_1	29 600	0.081	29 200	0.087	32 700	0.217	33 100	0.249
S_2	33 600	0.001	34 000	0.005	36 800	0.066	37 300	0.037
S_3	37 900	0.051	37 400	0.385	38 400	0.025	38 900	0.024
S_4	39 000	0.641	39 000	0.485	38 800*	0.000	39 200*	0.000
S_5	39 700	0.142	39 200*	0.018	39 200	0.031	40 000	0.132
S_6	39 800*	0.000	40 100	0.005	40 000	0.637	40 300	0.553
S_7	40 700	0.000	40 700	0.098	42 700	0.027	43 100	0.037
S_8	43 900*	0.002	43 000*	0.000	43 800	0.171	44 700	0.148
S_9	45 300	0.027	45 000	0.043	45 400	0.013	45 800	0.023

[a] The n → π* transitions are labelled with an asterisk, the other transitions are of the π → π* type.

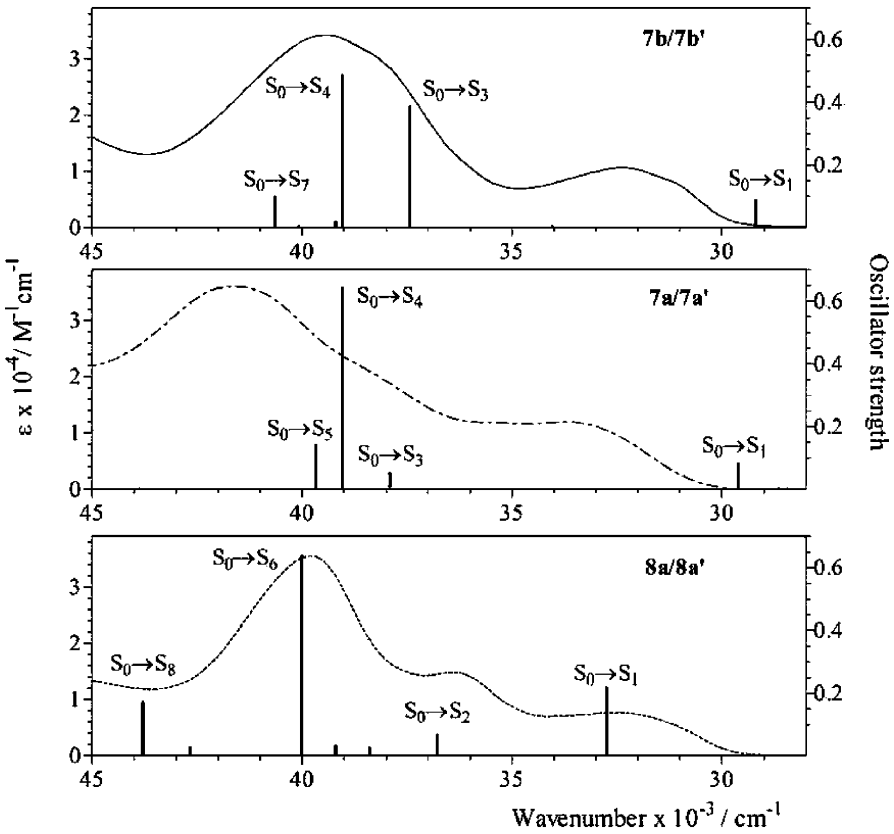

Fig. 1. Quantitative UV absorption spectra of **7a**, **b** and **8a** in CH_3CN. The stick-diagrams indicate the energies of the most intense singlet electronic transitions computed for compounds **7a**′ and **b**′ and **8a**′ in vacuum.

values for deprotonation of **7b** and **c** equal to 8.0 and 8.2, respectively, see Section 3.3).The choice of the solvents was limited by the insolubility of the compounds studied. The quantitative absorption spectra were recorded in CH_3CN and they are presented in Fig. 1.

The absorption spectrum of **7c** is almost identical with that of **7b** and it is not included in Fig. 1. The UV spectrum of **7a** in the spectral region $\nu^A < 45\,000\,cm^{-1}$ consists of two poorly separated, broad bands, of which the short-wavelength one peaking at $41\,840\,cm^{-1}$ is the most intense. The spectrum of **8a** in the same region shows three bands peaking at 39 680, 36 360 and $32\,470\,cm^{-1}$, which are similarly smooth and the intensity of the high energy band is almost equal to that of the respective peak in the spectrum of **7a**. The spectrum of **7b** is similar in terms of the number and intensity of the bands to that of compound **7a**. The similarity of the absorption spectra of both compounds suggests that the molecules **7b** in the ground state exist preferentially as N(5)*H* tautomer. The same tautomeric form was ascribed to the compound **2** (Scheme 1), which does not contain phenyl substituent at C(6) position, on the basis of a comparison of its absorption properties with those of respective model compounds [2].

The position of the absorption bands maximum in the spectra of **7a**–**c** and **8a** and the values of molar absorption coefficients are not significantly dependent on the polarity of the solvents used and are not sensitive to interactions with protic solvents. The relevant data characterising the absorption properties of the compounds studied: the position of the absorption bands maximum (ν^A_{max}) and full width at half maximum ($\Delta\nu^A_{1/2}$) of the lowest energy band in the solvents applied are presented in Table 2. High molar absorption coefficient values (ε_{max}, Fig. 1) and no significant solvatochromic effects indicate that for all compounds studied the long-wavelength absorption bands are related to the $\pi \rightarrow \pi^*$ transitions.

Comparing the absorption properties of compounds **7a**, **b** and **8a** with those of the compounds **1**–**6**, one can note that in general the attachment of an aromatic ring at the C(6) position of 9-oxo-imidazo[1,2-*a*]purine skeleton causes a red shift of the absorption maxima by $1100\,cm^{-1}$ (for **8a**) to $2410\,cm^{-1}$ (for **7b**) as a result of extension of the π electron system but it does not significantly change the bands intensity ($\nu^A_{max}(cm^{-1})$; ε_{max} ($M^{-1}\,cm^{-1}$)) in H_2O, compound **1**: 43 290 (27 300), 35 090 (10 100) [1]; compound **2**: 44 050 (34 400), 35 210 (11 900) [2]; compound **3**: 42 370 (34 700), 33 780 (8000) [6]; compound **4**: 42 190 (27 800), 37 780 (6500) [5]; compound **5**: 42 920 (27 400), 34 720 (12 100) [1]). The appended phenyl ring in **8a** exerts a more profound change because the peak at $36\,360\,cm^{-1}$ observed in Fig. 1 does not appear as a distinct band in the spectrum of a closely related compound **4**.

Table 2
Absorption (ν^{A}_{max}) and fluorescence (ν^{F}_{max}) maxima, full width at half maximum ($\Delta\nu_{1/2}$) and Stokes shift (S_s) for compounds **7a–c** and **8a** in selected solvents

Solvent	ν^{A}_{max} ($\times10^{-3}$ cm^{-1})	$\Delta\nu^{A}_{1/2}$ (cm^{-1})	ν^{F}_{max} ($\times10^{-3}$ cm^{-1})	$\Delta\nu^{F}_{1/2}$ (cm^{-1})	S_s (cm^{-1})	ν^{A}_{max} ($\times10^{-3}$ cm^{-1})	$\Delta\nu^{A}_{1/2}$ (cm^{-1})	ν^{F}_{max} ($\times10^{-3}$ cm^{-1})	$\Delta\nu^{F}_{1/2}$ (cm^{-1})	S_s (cm^{-1})
	7a					**7c**				
H_2O (pH 5.8)	41.67; 33.56	3400	25.97	5600	7590	39.84; 32.47	3400	25.64	5500	6830
CH_3CN	41.84; 33.44	3600	25.64	4400	7800	39.06; 32.26	3550	25.64	4800	6620
CH_3OH	41.67; 33.44	3400	26.67	4600	6770	39.22; 32.36	3800	25.97	5400	6390
n-C_4H_9OH	41.49; 33.44	3600	27.03	4000	6410	39.22; 32.15	3700	27.03	5000	5120
1,4-Dioxane	40.82; 33.00	3900	26.81	4000	6190	38.91; 31.75	3600	26.32	4800	5430
	7b					**8a**				
H_2O (pH 5.8)	40.00; 32.68	3400	25.64	5700	7040	40.16; 36.10; 32.68	4800	22.99	5600	9690
CH_3CN	39.37; 32.36	3600	25.32	5000	7040	39.68; 36.36; 32.47	3600	25.32	5600	7150
CH_3OH	39.68; 32.47	3400	25.64	5900	6830	40.00; 36.50; 32.47	4200	24.10	5600	8370
n-C_4H_9OH	39.22; 32.26	3700	27.17	5000	5090	39.68; 36.37; 32.36	3900	24.39	5600	7970
1,4-Dioxane	38.91; 31.85	3600	26.38	4700	5470	39.84; 36.63; 32.36	3700	25.00	6000	7360

The experimental absorption spectra of **7a**, **b** and **8a** in CH_3CN were compared with the energies (E_{calc}) of the most intense electronic transitions computed for respective molecules **7a′**, **b′** and **8a′** by the TD-DFT method (Fig. 1). A comparison of the absorption parameters, at least for the family of compounds without C(6) phenyl substituent (Scheme 1), showed that the nature of the N(3) substituent, e.g. hydroxyalkyl or ribosyl, had little effect on the absorption spectra. As shown in Fig. 1, for **8a**/**8a′** the computed energies of the most intense transitions ($S_0 \rightarrow S_1$, $S_0 \rightarrow S_2$, $S_0 \rightarrow S_6$) correspond very well to the location of the bands in the experimental absorption spectrum. For the pairs of compounds **7a**/**7a′** and **7b**/**7b′** the agreement between the calculated and experimental parameters is less profound, but still within the expected accuracy of TD-DFT(B3LYP/6-31G*) model (about 2000 cm^{-1}) the calculated transition energies and oscillator strengths give a good reproduction of the positions and relative intensity of absorption bands. In the compounds investigated mainly the $S_0 \rightarrow S_1$ transition is responsible for the intensity of the long-wavelength absorption band (Fig. 1).

The room temperature fluorescence spectra of compounds **7a**, **b** and **8a** in CH_3CN are displayed in Fig. 2. The shape of the emission curve of **7c** is identical with that of **7b** and it is not included for the sake of clarity.

All spectra consist of a single, structureless band with a maximum located in the same spectral region. For each compound the fluorescence excitation spectrum, the shape of the emission band, fluorescence quantum yield and decay kinetic in CH_3CN solution show no wavelength dependence. The fluorescence excitation spectrum of each compound coincides with the respective absorption spectrum. The fluorescence decay can be satisfactorily described by a monoexponential function. In respect to a possible tautomerism of **7b**, these results imply that the compound, both in the ground and lowest singlet excited state, exists as a single species identified as N(5)*H* tautomer. The relevant data characterising the emission spectral and photophysical properties of compounds **7a**–**c** and **8a** including: the position of the fluorescence band maximum (ν^{A}_{max}), full width at half maximum of the emission band ($\Delta\nu^{F}_{1/2}$), Stokes shift (S_s), fluorescence quantum yields (ϕ_F), lifetimes (τ_F), the rate constants of fluorescence (k_F) and radiationless processes (k_{NR}) calculated from the relations: $k_F = \phi_F/\tau_F$; $k_{NR} = (1 - \phi_F)/\tau_F$ are presented in Tables 2 and 3.

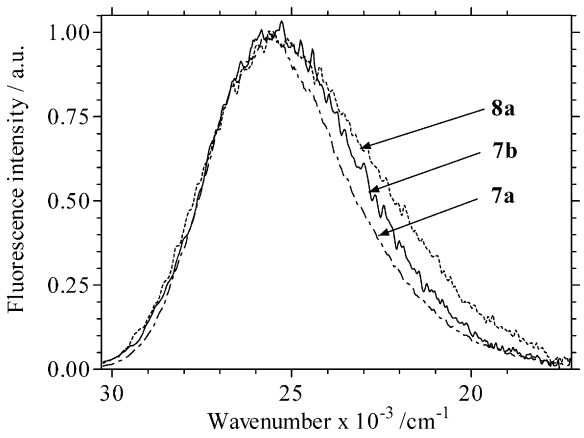

Fig. 2. Normalised fluorescence spectra of **7a**, **b** and **8a** in CH_3CN; $\nu_{exc} = 32\,260\,cm^{-1}$; room temperature.

The ϕ_F values measured for all the compounds in CH_3CN fall in the range $\phi_F = 0.078$–0.24 and **7c** is the most efficient fluorophore among the compounds studied (Table 3). The emission lifetimes also depend on the structure of the fluorophore and the determined τ_F values clearly show that the S_1 excited state of molecules **7a**–**c** in CH_3CN is about a factor of five longer lived than that of **8a**. A comparison of the rate constants included in Table 3 indicates that the short lifetime of **8a** is due not only to six times faster radiationless processes but also to three times higher fluorescence rate constant for this compound. On the other hand, the radiative rate constants, k_R, of the emitting state in CH_3CN calculated for molecules **7a**, **b** and **8a** from their absorption spectra using the modified Strickler and Berg relation [24], have similar values: $k_R = 9.1 \times 10^7$, 8.5×10^7 and $6.5 \times 10^7\ s^{-1}$ for molecules **7a**, **b** and **8a**, respectively. A significant reduction of k_F relative to k_R in the case of the compounds **7a** and **b** implies that the geometry of the molecules of these compounds undergo a significant change during the relaxation of the Frank–Condon excited state [24]. This is further supported by the TD-DFT calculation for the compound **7b′**. Partial geometry optimisation for the S_1 state of **7b′** indicates that the molecule becomes nearly planar in the excited state, with the torsional angle 7-6-1′-2-decreasing from 26° to 7° on going from S_0 to S_1 state.

A change of the solvent from acetonitrile to dioxane, alcohol or water (pH 5.8) influences the fluorescence parameters of the compounds, particularly those of **7a**–**c** (Tables 2 and 3). At the same time, the fluorescence measurements analogous to those described above for acetonitrile, prove that regardless of the solvent the ground state and the S_1 excited state of all the compounds studied consists of single species. These results support the ground state tautomeric homogeneity of **7b** and **c** in these media and enable the identification of the emitting species as a singlet excited N(5)*H* form of the molecules. The solvent effect common for compounds **7a**–**c** and **8a** manifests in their emission spectra as a batochromic shift of fluorescence band with increasing dielectric constant of a solvent (Table 2). The concomitant increase of the Stokes shift reflects a higher polarity of the molecules in the S_1 excited state than in the ground state. The other fluorescence parameters of **8a** do not depend significantly on the properties of the solvents applied. On the contrary, on changing solvents from less polar dioxane to water, the fluorescence quantum yields of **7a**–**c** are reduced by the factor ranging from 4 (for **7c**) to 10 (for **7a**). The reduction of ϕ_F is due to the decreasing fluorescence rate constant and increasing radiationless rate constant in polar solvents. The lowering of k_F value in polar solvents has been previously observed in several flexible systems (e.g. [25–27]). It

Table 3
Fluorescence quantum yields (ϕ_F)[a], lifetimes (τ_F), fluorescence (k_F) and nonradiative rate constants (k_{NR}) for compounds **7a–c** and **8a** in selected solvents

Solvent	ϕ_F	τ_F (ns)	k_F ($\times 10^{-7}$ s^{-1})	k_{NR} ($\times 10^{-8}$ s^{-1})	ϕ_F	τ_F (ns)	k_F ($\times 10^{-7}$ s^{-1})	k_{NR} ($\times 10^{-8}$ s^{-1})
	7a				**7c**			
H_2O (pH 5.8)	0.016	0.7	2.3	14.1	0.072	2.2	3.3	4.2
CH_3CN	0.13	5.5	2.4	1.6	0.24	6.6	3.6	1.2
CH_3OH	0.076	2.1	3.6	4.4	0.17	4.0	4.2	2.1
n-C_4H_9OH	0.11	2.7	4.1	3.3	0.20	3.4	5.8	2.4
1,4-Dioxane	0.16	3.9	4.1	2.2	0.30	4.9	6.1	1.4
	7b				**8a**			
H_2O (pH 5.8)	0.053	2.4	2.2	3.9	0.075	1.3	5.8	7.1
CH_3CN	0.17	6.2	2.7	1.3	0.078	1.0	7.8	9.2
CH_3OH	0.14	3.8	3.7	2.3	0.10	1.1	9.1	8.2
n-C_4H_9OH	0.17	3.2	5.3	2.6	0.12	1.5	8.0	5.9
1,4-Dioxane	0.25	4.7	5.3	1.7	0.086	1.3	6.6	7.0

[a] Estimated error: ±10%.

has been explained that this effect is a result of a molecular geometry change in the relaxed S_1 excited state which simultaneously diminishes a delocalisation of a charge [26].

It is also worth noting that the ϕ_F and τ_F values of **7b** do not change when the measurements of fluorescence quantum yields and lifetimes are performed in D_2O ($\phi_F(D_2O)/\phi_F(H_2O) = 1.08$, $\tau_F(D_2O)/\tau_F(H_2O) = 1.12$, at pD = pH 5.8). Thus, the phototautomerization frequently encountered in compounds containing the structural fragment N=C–NH (e.g. [28]) is not an important process in the S_1 excited state of **7b**.

3.3. pH dependent absorption and fluorescence properties of *7a–c*

The absorption and fluorescence properties of the molecules **7a–c** were studied in aqueous buffers solutions in the pH range 0–12. The spectral features of **8a** do not change within the pH range 4–12. Because of the instability of the compound its prototropic reactions have not been studied in more acidic solutions [5]. Fig. 3 (left) displays the absorption spectrum of **7b** recorded in a series of buffers with pH ranging from 5.8 to 12.

With increasing pH of the solution, the lowest energy absorption band gradually shifts to the red, a new band appears at $\nu^A = 35\,710\,cm^{-1}$ and the higher energy band becomes more intense. The spectra show isosbestic points at 31 750 and 33 840 cm^{-1} which are held over the whole basic pH range. The changes observed in the UV spectra in basic media are associated with the deprotonation of **7b** as shown in Scheme 3. The ground state equilibrium constant determined by spectrophotometric titration (Fig. 3 (left) inset) was found to be $pK_a = 8.0$.

For the samples of **7b** in buffers of pH 5.8–12.0 excited at the absorption isosbestic point ($\nu_{exc} = 31\,750\,cm^{-1}$) the series of fluorescence spectra presented in Fig. 3 (right) has been obtained. With increasing pH, the fluorescence intensity decreases and simultaneously the emission band maximum shifts towards longer wavelength. The red shifted emission ($\nu^F_{max} = 24\,690\,cm^{-1}$) is ascribed to the excited anion since its excitation spectrum (not shown) coincides with the absorption spectrum of the deprotonated molecule of **7b**.

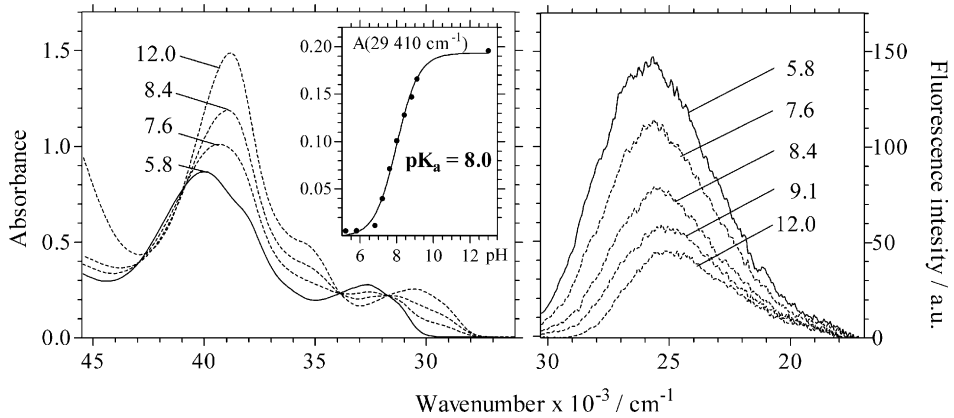

Fig. 3. UV absorption (left) and fluorescence spectra (right) of **7b** recorded at indicated pH; $\nu_{exc} = 31750\,cm^{-1}$. Inset left: the spectrophotometric titration curve for **7b**.

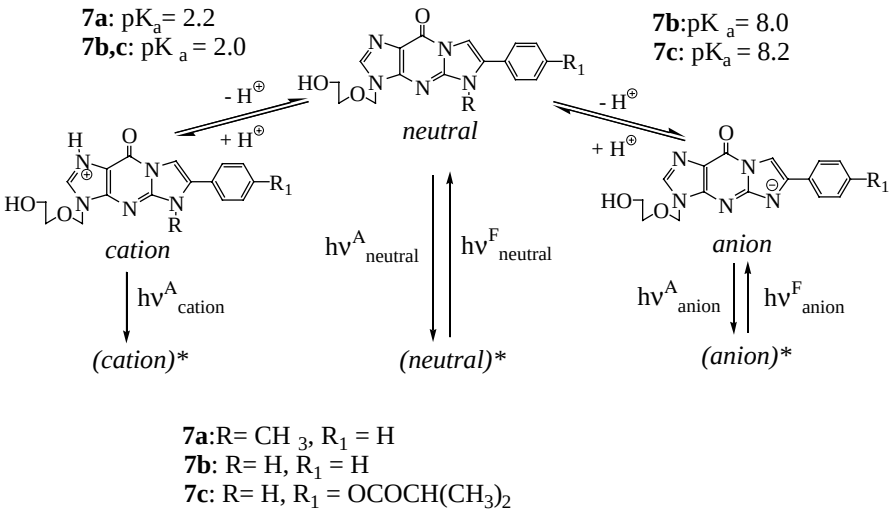

Scheme 3.

The spectral characteristics, the values of ϕ_F and τ_F, of the ionic species are presented in Table 4. The fluorescence of the anion formed from **7b** is about four times less efficient and shorter lived than that of the neutral molecule.

The spectrofluorimetric titration curve I_0^F/I_F versus pH (not shown) constructed from the changes in the fluorescence intensity of the neutral molecule of **7b** (I_F at $\nu_{max}^F = 29\,410\,cm^{-1}$; I_0^F refers to the value measured at pH 4–6, where it remains constant) has an inflection point precisely at pH 8.1. This value is within an experimental error (±0.1) identical to pK_a found for the ground state neutral molecule–anion equilibrium of **7b**. On the other hand the estimation of the acidity constant in the S_1 state, by Förster cycle method [29] using the relation [30]:

$$pK_a^* = pK - \frac{0.625}{T}(\nu_{00}^{HA} - \nu_{00}^{A^-})$$

where ν_{00} is wavenumber of electronic transitions in the neutral form (HA) and anionic form (A^-) calculated from absorption and fluorescence spectra: $\nu_{00} = (\nu_{max}^A + \nu_{max}^F)/2$ at $T = 293\,K$, gave the value $pK_a^* = 4.8$ for **7b** in the S_1 state. The divergent values obtained from spectrofluorimetric titration and Förster method indicates that deprotonation of **7b** in the excited S_1 state does not occur because of the short lifetime of the excited species. Thus, the fluorescence intensity changes presented in Fig. 3 (right) reflect only the ground state equilibrium of **7b**. This interpretation correlates with the measurements of fluorescence lifetimes. In contrast to the results obtained in aqueous solution at pH 5.8, in the pH range 7.0–9.0 the fluorescence decay kinetic of **7b** is wavelength dependent. At $\nu^F = 29\,410\,cm^{-1}$, where only the neutral form emits the decay is monoexponential with the lifetime $\tau_F = 2.4\,ns$ while at $\nu^F = 22\,220\,cm^{-1}$ a short-lived component is needed to obtain good fit (pH = 8.0, τ_F = 2.4 ns, rel. ampl. 0.85 and $\tau_F = 0.8\,ns$, rel. ampl. 0.15). At pH 10 when **7b** in the ground state exists almost exclusively in the deprotonated form the fluorescence band is red shifted (Table 4) and the emission at $\nu^F = 29\,410\,cm^{-1}$ is not observed. Under these conditions the decay of the fluorescence at $\nu^F = 22\,220\,cm^{-1}$ is monoexponential and the lifetime of the excited anion $\tau_F = 0.8\,ns$ (Table 4) was determined from the analysis of the decay curve. Thus, the longer lived component of the fluorescence of **7b** in buffer solution at pH 8 found from the analysis of the biexponential decay measured at $\nu^F = 22\,220\,cm^{-1}$, i.e. in the spectral region where both the neutral molecule and the anion emit, can be ascribed to the excited neutral molecule **7b** and the short-lived component to the corresponding excited anionic species.

The changes in the absorption and fluorescence spectra of **7c** in basic solutions (pK_a = 8.2 from spectrophotometric titration) resemble those described above for **7b** (Table 4). The absorption and fluorescence spectra, ϕ_F and τ_F values

Table 4
Absorption (ν_{max}^A, ε) and fluorescence (ν_{max}^F, ϕ_F, τ_F) parameters for ionic species derived from compounds **7a**–**c** in aqueous buffers solutions

pH	Compound	ν_{max}^A ($\times 10^{-3}\,cm^{-1}$) (ε, ($M^{-1}\,cm^{-1}$))	ν_{max}^F ($\times 10^{-3}\,cm^{-1}$)	ϕ_F[a]	τ_F (ns)
0	**7a** cation	40.82 (31 820); 38.46 (sh, 27 840); 32.47 (9940)	–	–	–
10	**7b** anion	38.76 (58 800); 35.71 (sh, 20 390); 30.58 (10 190)	24.69	0.013	0.8
0	**7b** cation	39.84 (26 550); 38.17 (27 200); 31.75 (9640)	–	–	–
10	**7c** anion	38.61 (45 570); 35.71 (sh, 18 800); 30.49 (8060)	25.00	0.008	<0.5
0	**7c** cation	39.53 (24 200); 37.59 (27 800); 31.75 (10 300)	–	–	–

sh: shoulder.
[a] Estimated error: ±10%.

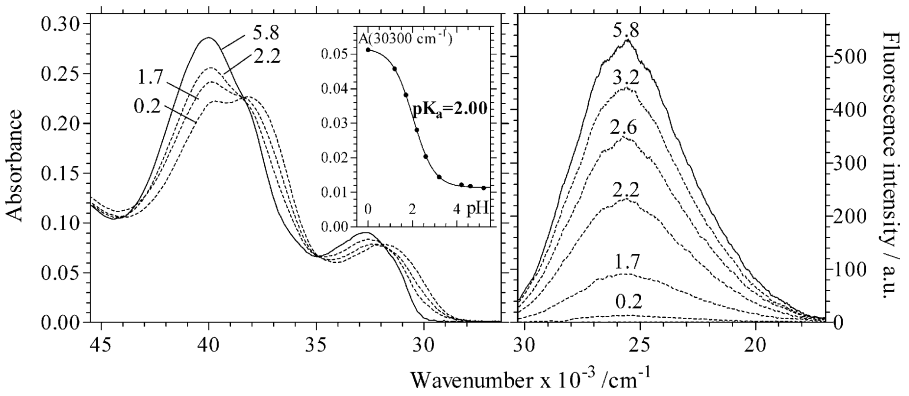

Fig. 4. UV absorption (left) and fluorescence spectra (right) of **7b** recorded at indicated pH; $\nu_{exc} = 31\,950\,cm^{-1}$ (absorption isosbestic point). Inset left: the spectrophotometric titration curve for **7b**.

for compound **7a**, which does not have dissociable hydrogen atom, remain unchanged on going from neutral to basic media (pH 6–12), as expected.

The series of the absorption spectra of **7b** in acidic solutions are presented in Fig. 4 (left).

The pH induced spectral changes observed for **7a** and **c** are very similar (Table 4). In all cases the spectral changes are compatible with the assumption of two component equilibrium containing a neutral molecule and a cation (Scheme 3). The pK_a values characterising the ground state neutral molecule–cation equilibrium determined from the absorption spectra are pK_a = 2.0. for **7b** and **c** and pK_a = 2.2 for **7a**. For the molecules of **7** in the ground state, the preferred site of protonation is nitrogen N(1). As shown by B3LYP/6-31G* calculations for the compound **7b′**, the cation with proton attached to N(1) atom is more stable than any other of its isomers. For example, the cations with protons attached to N(4) or N(8) atoms are more than 15 kcal/mol higher in energy.

The corresponding changes observed in the fluorescence spectra are illustrated for **7b** in Fig. 4 (right). With increasing acid concentration the fluorescence intensity decreased and no new emission appeared. The spectrofluorimetric titration curves constructed from the intensity changes at $\nu^F = 28\,570\,cm^{-1}$ have inflection points at pH 2.2 for **7b** and **c** and at 2.3 for **7a**, and these values correspond almost exactly to the ground state pK_a values. The lifetimes determined from the monoexponential fluorescence decays of **7a**–**c** remain unchanged irrespective of the monitored ν^F and acidity of the medium confirming that no excited state reaction occurs and the cationic species derived from the compounds are non-fluorescent.

Acknowledgements

This work was supported by the Polish Committee for Scientific Research (KBN) grant no. PBZ-KBN-059/T09/18. The calculations were performed at the Poznan Supercomputer Center (PCSS).

References

[1] J. Boryski, B. Golankiewicz, E. De Clercq, J. Med. Chem. 31 (1988) 1351.
[2] P.D. Sattsangi, N.J. Leonard, C.R. Frihart, J. Org. Chem. 42 (1977) 3292.
[3] M.K. Dosjanjh, A. Chenna, E. Kim, H. Fraenkel-Conrat, L. Samson, B. Singer, Proc. Natl. Acad. Sci. USA 91 (1994) 1024.
[4] U.L. RajBhandary, S.H. Chang, A. Stuart, R.D. Faulkner, R.M. Hoskinson, H.G. Khorana, Proc. Natl. Acad. Sci. USA 57 (1967) 751.
[5] B. Golankiewicz, T. Ostrowski, J. Boryski, E. De Clercq, J. Chem. Soc. Perkin Trans. 1 (1991) 589.
[6] T. Itaya, H. Matsumoto, T. Watanabe, T. Harada, Chem. Pharm. Bull. 33 (1985) 2339.
[7] T.M. Nordlund, R. Rigler, C. Glemarec, J.-C. Wu, H. Bazin, G. Remaud, J. Chattopadhyaya, Nucleosides Nucleotides 7 (1988) 805.
[8] H. Kasai, M. Goto, K. Ikeda, M. Zama, Y. Mizuno, S. Takemura, S. Matsuura, T. Sugimoto, T. Goto, Biochemistry 15 (1976) 898.
[9] H. Kasai, M. Goto, S. Takemura, T. Goto, S. Matsuura, Tetrahedron Lett. (1971) 2725.
[10] E.M. Evleth, D.A. Lerner, Photochem. Photobiol. 26 (1977) 103.
[11] J.R. Lakowicz, Principles of Fluorescence Spectroscopy, second ed., Kluwer Academic Publishers, Plenum Press, New York, 1999, pp. 16 and 206.
[12] J. Balzarini, T. Ostrowski, T. Goslinski, E. De Clercq, B. Golankiewicz, Gene Ther. 9 (2002) 1173.
[13] B. Golankiewicz, T. Ostrowski, G. Anderi, R. Snoeck, E. DeClercq, J. Med. Chem. 37 (1994) 3187.
[14] T. Ostrowski, J. Zeidler, T. Goslinski, B. Golankiewicz, Nucleosides Nucleotides Nucleic Acids 19 (2000) 1911.
[15] T. Goslinski, B. Golankiewicz, E. De Clercq, J. Balzarini, J. Med. Chem. 45 (2002) 5052.
[16] T. Goslinski, G. Wenska, B. Golankiewicz, J. Balzarini, E. DeClercq, Nucleosides Nucleotides Nucleic Acids 22 (2003) 911.
[17] D.D. Perrin, B. Dempsey, Buffers for pH and Metal Ion Control, Chapman and Hall, New York, 1979, p. 123.
[18] A. Albert, E.P. Serjeant, The Determination of Ionization Constants, Chapman and Hall, New York, 1984, p. 70.
[19] E. Gross, J. Dobson, M. Petersilka, Top. Curr. Chem. 181 (1996) 81.
[20] A. Becke, J. Chem. Phys. 98 (1993) 5648.
[21] R. Ditchfield, W.J. Hehre, J.A. Pople, J. Chem. Phys. 54 (1971) 724.
[22] M.J. Frisch, G.W. Trucks, H.B. Schlegel, G.E. Scuseria, M.A. Robb, J.R. Cheeseman, J.A. Montgomery, Jr., T. Vreven, K.N. Kudin, J.C. Burant, J.M. Millam, S.S. Iyengar, J. Tomasi, V. Barone, B. Mennucci, M. Cossi, G. Scalmani, N. Rega, G.A. Petersson, H. Nakatsuji, M. Hada, M. Ehara, K. Toyota, R. Fukuda, J. Hasegawa, M. Ishida, T. Nakajima, Y. Honda, O. Kitao, H. Nakai, M. Klene, X.

Li, J.E. Knox, H.P. Hratchian, J.B. Cross, C. Adamo, J. Jaramillo, R. Gomperts, R.E. Stratmann, O. Yazyev, A.J. Austin, R. Cammi, C. Pomelli, J.W. Ochterski, P.Y. Ayala, K. Morokuma, G.A. Voth, P. Salvador, J.J. Dannenberg, V.G. Zakrzewski, S. Dapprich, A.D. Daniels, M.C. Strain, O. Farkas, D.K. Malick, A.D. Rabuck, K. Raghavachari, J.B. Foresman, J.V. Ortiz, Q. Cui, A.G. Baboul, S. Clifford, J. Cioslowski, B.B. Stefanov, G. Liu, A. Liashenko, P. Piskorz, I. Komaromi, R.L. Martin, D.J. Fox, T. Keith, M.A. Al-Laham, C.Y. Peng, A. Nanayakkara, M. Challacombe, P.M.W. Gill, B. Johnson, W. Chen, M.W. Wong, C. Gonzalez, J.A. Pople, Gaussian 03, Revision B.3, Gaussian, Inc., Pittsburgh, PA, 2003.

[23] S.R. Meech, D. Phillips, J. Photochem. 23 (1983) 193.
[24] S.J. Strickler, R.A. Berg, J. Chem. Phys. 37 (1962) 814.
[25] G. Haucke, P. Czerney, C. Igney, H. Hartmann, Ber. Bunsen-Ges. Phys. Chem. 93 (1989) 805.
[26] M. Belletete, G. Durocher, J. Phys. Chem. 96 (1992) 9183.
[27] S.K. Saha, S.K. Dogra, J. Photochem. Photobiol. A: Chem. 110 (1997) 257.
[28] P. Avours, L.L. Yang, M. Asharf El-Bayoumi, Photochem. Photobiol. 24 (1976) 211.
[29] T. Förster, Z. Electrochem. Angew. Phys. Chem. 54 (1950) 42.
[30] B. Marciniak, H. Kozubek, S. Paszyc, J. Photochem. 28 (1985) 529.